A Well Collimated Quasi-Continuous Atom Laser

E.W. Hagley[1], L. Deng[1,2], M. Kozuma[3], J. Wen[1], K. Helmerson[1], S.L. Rolston[1], and W. D. Phillips[1].

[1]National Institute of Standards and Technology, Gaithersburg, MD 20899. [2]Georgia Southern University, Statesboro, GA 30460. [3]Institute of Physics, University of Tokyo, Tokyo 153-8902, Japan.

January 27, 1999

Extraction of sodium atoms from a trapped Bose-Einstein condensate (BEC) using a coherent, stimulated Raman process is demonstrated. Optical Raman pulses drive transitions between trapped and untrapped magnetic sublevels, giving the output-coupled BEC fraction a well defined momentum. The pulsed output coupling can be run at such a rate that the extracted atomic wave packets strongly overlap, forming a highly-directional, quasi-continuous matter wave.

The occupation of a single quantum state by a large number of identical bosons (*1-5*) is a matter-wave analog to the storage of photons in a single mode of a laser cavity. Just as one extracts a coherent, directed beam of photons from a laser cavity using a partially transmitting mirror as an output coupler, one can analogously extract directed matter waves from a condensate. Such a source of matter waves, or "atom laser," is important in the field of atom optics (*6*), the manipulation of atoms analogous to the manipulation of light. Its development is providing atom sources as different from ordinary atomic beams as lasers are from light bulbs.

The first demonstration of a BEC output coupler was reported in 1997 (*7*), where coherent, rf-induced transitions were used to change the internal state (magnetic sublevel) of the atoms from a trapped to an untrapped one. This method, however, did not allow the direction of the output-coupled atoms to be chosen. The extracted atoms fell under the influence of gravity and expanded because of their intrinsic repulsion. We demonstrate a highly-directional method to optically couple out a variable fraction of a condensate, and apply this method to produce a well collimated, quasi-continuous beam of atoms, an important step toward a truly cw atom laser (*8*).

Our output coupling is based on stimulated Raman transitions between magnetic sublevels (*9,10*). The sublevel into which the atoms are transferred is unaffected by the trapping potential and the process imparts a well defined momentum to the output-coupled condensate fraction. In contrast, previous work on Bragg diffraction (*11*) transferred momentum without changing the internal state of the atom. A single Raman pulse can couple out any desired fraction of the condensate. By changing the angle between the wavevectors $\vec{k}$ of the Raman lasers ($k = 2\pi/\lambda$, $\lambda = 589\,\text{nm}$) and using higher order ($2n$-photon) Raman transitions, it is possible to impart any momentum of magnitude 0 to $2n\hbar k$ (*11*) to the atoms (for sodium, $2\hbar k$ corresponds to a velocity of 6 cm/s). In this way it is possible to choose the energy of the extracted deBroglie wave, producing a widely-tunable atom laser.

In the present experiment a hybrid evaporation technique using a Time Orbiting Potential (TOP) trap (*12, 13*) is employed to form a sodium condensate (*11*). We typically obtain a condensate, without a discernible normal fraction, with about 10^6 atoms in the $3S_{1/2}, F=1, m=-1$ state (*14*). Once the condensate is formed we adiabatically expand the trapping potential in $0.5\,\mathrm{s}$, reducing the trapping frequencies to $\omega_x/2\pi$ = 18 Hz, $\omega_y/2\pi$ = 25 Hz and $\omega_z/2\pi$ = 35 Hz. We have measured (*15*) that our adiabatic cooling reduces the asymptotic rms momentum width of the released condensate to $0.09(1)\hbar k$ (*16*).

In Raman output coupling (Fig. 1), a moving standing wave, composed of two nearly counter-propagating laser beams with a frequency difference $\delta = \omega_2 - \omega_1$ (*17*), is applied to the condensate for a short period of time. These beams propagate nearly along the $\hat{z}$-axis of the trap (gravity is along $\hat{x}$) and each beam is detuned from the $3S_{1/2}, F=1 \rightarrow 3P_{3/2}, F'=2$ transition by $\Delta/2\pi = -1.85\,\mathrm{GHz}$ to suppress spontaneous emission. A stimulated Raman transition occurs when an atom changes its state by coherently exchanging photons between the two laser beams (absorption from ω_1 and stimulated emission into ω_2). The atom acquires momentum $\vec{P} = \hbar(\vec{k}_1 - \vec{k}_2) = P\hat{z}$ (in our case) with $P = 2\hbar k \sin(\theta/2)$ (*18*). Therefore, an atom initially at rest acquires a kinetic energy $\hbar\delta_{\mathrm{Recoil}} = P^2/(2M)$, where M is the atomic mass. The stimulated Raman process can change the internal energy state of an atom by driving $\Delta m = 1$ or even $\Delta m = 2$ transitions (*19*). The energy difference between the absorbed and emitted photons must account for both the change in kinetic energy and any change in the internal (magnetic) energy level of the atom: $\hbar\delta = \hbar\delta_{\mathrm{Zeeman}} - \hbar\delta_{\mathrm{recoil}}$. By changing the internal state of trapped atoms to $m = 0$, a state that feels no trapping forces, we release the atoms and impart a momentum that kicks them away.

Our Raman output coupling scheme dramatically reduces the transverse momentum width of the extracted atoms compared to other methods such as rf output coupling (*7*). The $0.09(1)\hbar k$ rms momentum width discussed previously corresponds to the average release energy of $2/7\mu$ (the chemical potential $\mu \propto N^{2/5}$, where N is the number of atoms in the condensate) per atom caused by the intrinsic repulsion between the atoms. If, however, only a small number of atoms is coupled out of the condensate into the $m = 0$ state, the average energy per extracted atom is two times larger (*20*). For atoms coupled out of a spherically symmetric trap without an initial momentum kick, this release energy causes an isotropic momentum spread. In our case, where significant momentum is imparted to the atoms, the release energy is primarily channeled into the forward direction. This dramatically reduces the transverse rms momentum width, resulting in a highly collimated output beam. The transverse momentum width (*21*) is reduced by roughly the ratio of the characteristic time it takes the output-coupled atoms to leave the still-trapped condensate, divided by the timescale over which the mean field repulsion acts on the freely expanding condensate (*22*) and will therefore be extremely small compared to its longitudinal momentum of $2\hbar k$. This has been confirmed by numerical calculations which estimate the mean field component of the transverse rms momentum width to be 0.004 $\hbar k$.

The uncertainty principle imposes an additional transverse momentum width of $0.002\hbar k$ due to the finite size of our condensate. The predicted mean-field momentum width is close to this lower limit and corresponds to a divergence of a few milliradians, comparable to that of a typical commercial optical laser. As this momentum width is so small, it is difficult to measure experimentally (during the typical 7 ms duration of the experiment the radius of the atomic cloud would only expand 1 μm).

To implement this Raman output coupling scheme requires that special attention be paid to the time-varying magnetic field in the TOP trap. In the presence of gravity the atoms sag (in our case about 0.8 mm) away from the center of the trap to a position where the magnitude of the magnetic field changes as the bias field rotates (*23*). The time dependent detuning for the two-photon transition is:

$$\delta(t) = \frac{\Delta m \mu_B}{2\hbar} \left| \vec{B}(t) \right| - \frac{2\hbar k^2 \sin^2(\theta/2)}{M}, \qquad (1)$$

where μ_B is the Bohr magneton and Δm = 0, 1, or 2. The frequency difference between $m = -1$ and $m = 0$ sublevels changes by nearly 4 MHz as the TOP field rotates. This frequency difference is large compared to the effective width of the transition, the inverse of the Raman pulse length (typically 6 μs). Therefore, the Raman pulse is synchronized to the maximum of $\delta(t)$ to minimize variations in the resonance frequency during the transition. Compared to continuous output coupling, this pulsed Raman output coupling results in less spontaneous emission for the same percentage of output-coupled atoms.

When the Raman pulses were applied, the magnetic field direction was along the $\hat{x}$-axis (vertical), as was the polarization of one of the two Raman lasers (which only drove $\Delta m = 0$ (π) transitions). This laser had an intensity of $300\,\mathrm{mW/cm^2}$ (*24*). The second Raman laser drove Δm=1 (σ) transitions when its polarization was along $\hat{y}$. It had an intensity of $600\,\mathrm{mW/cm^2}$ but only half of this power was useful due to selection rules. For $\Delta / 2\pi = -1.85$ GHz, this intensity corresponds to an average time per atom between spontaneous emission events of 70 μs.

Directional output coupling is observed by imaging the atoms several milliseconds after the Raman pulse. Figure 2 shows optical depth images obtained by first optically pumping the atoms to the $3S_{1/2}, F = 2$ state, then absorption-imaging (*2*) on the $3S_{1/2}$, F=2$\rightarrow 3P_{3/2}$, F'=3 transition. The sequence (Figs. 2A-C) shows a BEC ($F = 1, m = -1$), followed by two BECs after the application of a single Raman pulse. The TOP trap confining fields were held on for 7 ms after applying the Raman pulse before being switched off. The system was then allowed to evolve freely for 1.6 ms before being imaged. Notice that the position of the output-coupled atoms in Fig. 2B is different from that of Fig. 2C. In the former, the atoms that have undergone the Raman transition are in the state $m = 0$ and therefore no longer feel the trapping potential, whereas in Fig. 2C the atoms are still trapped. The position of the $m = 0$ atoms corresponds to free-flight with momentum $2\hbar k\hat{z}$ during the entire 8.6 ms whereas the position of the atoms in Fig. 2C corresponds to their classical turning point in the trap (7 ms is approximately one quarter of the 28.6 ms oscillation period along $\hat{z}$).

In the case where the detuning of the lasers from the excited state is large compared to the excited-state hyperfine structure splitting, it is not possible to drive $\Delta m = 2$ transitions directly with two photons because the ground state acts like a spin 1/2 system for which there are only two states. Instead, we can couple to the $m = +1$ state by combining the Raman process with Majorana transitions due to the TOP rotating magnetic field zero (*13*). Atoms were first output-coupled to the m=0 state and imaged 10.6 ms later after having crossed the orbit of the zero of the magnetic field (*27*), known as the "circle of death", which orbits in the $\hat{x}$-$\hat{z}$ plane (Fig. 2D). For this image the rotating bias field was reduced by a factor of 3, reducing the distance to the orbiting magnetic field zero to 0.3 mm. As the atoms crossed this orbit they lost their quantization axis and were repeatedly projected to all three magnetic sublevels at the 20 kHz TOP frequency. The atoms in $m = -1$, 0, and +1 states were respectively retarded, unimpeded, and ejected by the trapping potential, giving rise to three spatially separated stripes of atoms. At the time of imaging, the atoms that ended in the $m = -1$ state have already been pulled back to the circle of death by the trap.

Although it is not possible to drive the $\Delta m = 2$ transition with two photons, it is possible with four using the $m = -1 \rightarrow m = 0 \rightarrow m = +1$ transition scheme (Fig. 3C). A single 6 μs Raman pulse with $\delta / 2\pi = 6.15$ MHz and the same intensities used for Fig. 2B was applied. In Fig. 3A, the TOP was switched off immediately after the Raman pulse and the atoms imaged 5.6 ms later. The $m = +1$ atoms received $4\hbar k\hat{z}$ of momentum from four photons, while the $m = 0$ atoms received only $2\hbar k\hat{z}$ from two photons; thus the $m = +1$ atoms moved twice as far as the $m = 0$ atoms. With the TOP switched off 4 ms after the Raman pulse and the system imaged 1.6 ms later (Fig. 3B), the atoms in the $m = +1$ anti-trapped state are accelerated away from the trap, causing them to move further.

To produce quasi-continuous output coupling we used multiple Raman pulses. The laser intensities were reduced and the detuning was again chosen to be $\delta/2\pi$ = 6.4 MHz to couple primarily to the $m=0$ state. For the optical depth images of the condensate after one, three and six Raman pulses (Figs. 4A-C), the TOP was held on for a 9 ms window during which time 6 μs Raman pulses were fired at a subharmonic of the rotating bias frequency. The magnetic fields were then extinguished and the atoms imaged 1.6 ms later. The intensity of the laser whose polarization was aligned with $\hat{x}$ was 300, 150, and 100 $\mathrm{mW/cm^2}$, respectively, in order to couple out different fractions of the condensate (the intensity of the second Raman laser was twice that of the first).

In Fig. 4D the TOP trap was held on during a 7 ms window during which time 140 Raman pulses were fired at the 20 kHz frequency of the rotating bias field and the distribution of atoms was imaged 1.6 ms later. The Raman pulse duration and intensity were reduced to 1 μs and 40 $\mathrm{mW/cm^2}$ for Fig. 4D, to ensure that the total integrated pulse time of 140 μs was much less than the spontaneous emission time of ~500 μs. The phase of the output-coupled matter wave evolves at ~100 kHz with respect to the condensate itself due to the kinetic energy imparted by the two-photon Raman transition (*28*). Since 100 kHz is an integer multiple of the ~ 20 kHz output coupling repetition rate, the interference of successive pulses is almost completely constructive (*29*). In the time between two Raman pulses each output-coupled wave packet moves only 2.9 μm, much less than the ~50 μm size of the condensate, so the output-coupled atoms form a quasi-continuous coherent matter wave. By varying the delay between pulses, the interference between output-coupled wavepackets can be used to investigate the coherence properties of the condensate.

It is apparent that there is also coupling to the m=+1 state in Fig. 4D because some output-coupled atoms have moved the distance that an atom with momentum $4\hbar k\hat{z}$ moves in 8.6 ms. Such coupling to the m=+1 state occurs in this case because the spectral width of the 1 μs Raman pulse is sufficiently broad (*30*) to drive a transition from the state m=0 (momentum $2\hbar k\hat{z}$) to the state *m*=+1 (momentum $4\hbar k\hat{z}$). In our experiment the trajectories of the two output-coupled beams (*m*=0 and *m*=+1) are spatially separated because the direction of momentum transfer is orthogonal to gravity. These two beams appear to overlap in Fig. 4D because the camera views them from above. Coupling to the *m*=+1 state could be suppressed by using a larger bias magnetic field and a larger detuning Δ to exploit the second-order Zeeman shift, and to reduce the pulse bandwidth without excessive spontaneous emission. To completely suppress coupling to unwanted anti-trapped states a Raman transition to the *F*=2, *m*=0 ground state of Na could be used.

An important property of the condensate, and any output-coupled fraction, is its coherence. Coherence effects between two condensates have already been observed by dropping them and allowing them to interfere (*31*). Because we use a stimulated Raman process, our output beam should be fully coherent. The effect of the mean field on the atoms as they leave the BEC will be to distort the outgoing wave without resulting in any true loss of coherence. In a separate experiment we observed matter-wave interference due to the 100 kHz phase evolution discussed above and we are using it to measure the coherence properties of the condensate.

References and Notes

1. A. Einstein, Sitzungsber. Kgl. Preuss. Akad. Wiss. 261, (1924); ibid. 3, (1925).
2. M.H. Anderson, J.R. Ensher, M.R. Matthews, C.E. Wieman, and E.A. Cornell, Science, **269**, 198 (1995).
3. K.B. Davis et al., Phys. Rev. Lett. **75**, 3969 (1995).
4. C.C. Bradley, C.A. Sackett, and R.G. Hulet, Phys. Rev. Lett. **78**, 985 (1997). See also, C.C. Bradley, C.A. Sackett, J.J. Tollett, and R.G. Hulet, Phys. Rev. Lett. **75**, 1687 (1995).
5. D.G. Fried et al., Phys. Rev. Lett. **81**, 3807 (1998).
6. Journal De Physique, **4**, 11 (1994); Appl. Phys. B. **54**, 321 (1992); J. Phys. Rep., **240** (1994) (special issues on Optics & Interferometry with Atoms).
7. M.-O. Mewes et al., Phys. Rev. Lett., **78**, 582 (1997).
8. A truly cw atom laser produces a continuous, coherent matter wave output while being continuously replenished with new atoms, in direct analogy with a cw optical laser. The coherence length of such a laser would be longer than the size of the trapped condensate just as the coherence length of a cw optical laser is longer than the laser cavity.
9. G. Moy, J. Hope, and C. Savage, Phys. Rev. A **55**, 3631-3638 (1997).

10 M.A. Edwards, C.W. Clark, K. Burnett, S.L. Rolston, and W.D. Phillips, (accepted, J. Phys. B).

11. M. Kozuma et al., Phys. Rev. Lett. **82**, (1999).
12. Our TOP trap is different from previous TOP traps (13) because the rotating bias field orbits in a plane that includes the quadrupole axis. The field gradient along the quadrupole axis ($\hat{z}$) is 9.2 T/m, and the rotating bias field is 1.0 mT. The time averaged magnetic field forms a trap with harmonic frequencies $\omega_x/2\pi$ = 180 Hz, $\omega_y/2\pi$ = 250 Hz and $\omega_z/2\pi$ = 360 Hz.

13. W. Petrich, M.H. Anderson, J.R. Ensher, and E.A. Cornell, Phys. Rev. Lett. **74** 3352 (1995).

14. Atoms in the state $m=-1$ are trapped by the magnetic fields whereas those in state $m=+1$ are anti-trapped. The state $m=0$ does not feel the confining potential of the magnetic trap.

15. This was done by switching off the trap and measuring the rate of the mean-field-driven ballistic expansion of the condensate at long times (>10 ms).

16. All uncertainties reported in this paper are one standard deviation combined statistical and systematic uncertainties.

17. For frequency stability, both beams are derived from a single dye laser with the frequency difference controlled by two acousto-optic modulators.

18. θ, which equals 166° in our case, is the angle between $\vec{k}_1$ and $\vec{k}_2$, and $|\vec{k}_1| \approx |\vec{k}_2| = k$. Therefore $P = 1.99\hbar k \approx 2\hbar k$.

19. We define $\Delta m = m_{\text{final}} - m_{\text{initial}}$. $m_{\text{initial}} = -1$ is the only magnetically trapped state.

20. Assuming the scattering lengths among all *m*-states are the same, this can be derived from expressions found in, F. Dalfovo, S. Giorgini, L. P. Pitaevskii, S. Stringari, Rev. Mod. Phys. **71**, (2) (1999). The energy needed to add one atom is μ, which has a magnetic contribution of $3/7\mu$ and a mean-field contribution of $4/7\mu$. If a small number of atoms are output-coupled to $m=0$, a state that is not magnetically trapped, their release energy will simply be $4/7\mu$, or twice the average release energy of $2/7\mu$ for the whole condensate.

21. In addition, the longitudinal momentum width is reduced by roughly the same factor due to kinematic compression.

22. The characteristic time during which the mean field potential energy turns into kinetic energy in the released BEC is $1/\overline{\omega}$ (in our case about 6 ms), where $\overline{\omega}$ is the geometric mean of the three trapping frequencies. For our two-photon Raman

transition the characteristic time scale for leaving the region of the condensate is 300 μs.

23. This is because our TOP field rotates in $\hat{x}$-$\hat{z}$ plane which includes the direction of gravity.

24. The power quoted was the average over a 3 mm diameter aperture in the center of a somewhat inhomogeneous 7 mm beam. These powers were empirically chosen to produce good output coupling.

25. The resonance frequency, for the Δm = 2 four-photon transition discussed later, was found to be 6.15(5) MHz, in good agreement with the calculated value of 6.0(2) MHz based on measurements of the trapping magnetic fields. This additional detuning of 2×250 kHz = 500 kHz from the four-photon resonance frequency is large compared to the Fourier width of the Raman pulse and results in a suppression of coupling to the $4\hbar k\hat{z},\ m=+1$ state.

26. A stimulated Raman transition that changes the momentum state of an atom but does not change the internal energy state can be viewed as Bragg diffraction (11). See also, P.J. Martin, B.G. Oldaker, A.H. Miklich, and D.E. Pritchard, Phys. Rev. Lett. **60**, 515 (1988).

27. Due to our choice of applying the Raman beams along the quadrupole axis of the trap ($\hat{z}$), the trajectory of the output-coupled atoms (initially along $\hat{z}$) lies in the $\hat{x}$-$\hat{z}$ plane because gravity is along $\hat{x}$. This is the plane of the rotating magnetic field zero and so the atoms will, at some point in time, cross this "circle of death" (actually an ellipse).

28. In the case of $\theta=180^\circ$ the recoil momentum from a first-order Raman transition is exactly $2\hbar k\hat{z}$, which corresponds to a frequency of 100.1 kHz.

29. This was confirmed in a separate experiment which looked at the interference of two clouds of atoms diffracted out of the condensate.

30. If the output coupling process were made continuous, by using an optical dipole or

magnetic trap with no time dependent magnetic fields, such coupling would not occur because the Fourier width of the light pulse could be made arbitrarily small. It would therefore be a simple matter to make a continuous Raman output coupler in such a case.

31. M.R. Andrews et al., Science **273**, 637 (1997).

32. We thank C.W. Clark, M.A. Edwards, and P.S. Julienne for their valuable comments and suggestions. M.K. acknowledges the support of the Japanese Society for the Promotion of Science for Young Scientists. This work was supported in part by the Office of Naval Research and NASA.

Figure Captions

Fig. 1 Principle of the Raman output coupler. Energy conservation requires a relative detuning, $\delta = \omega_2 - \omega_1$, between the Raman lasers. Total energy as a function of atomic momentum is plotted, where the parabolas correspond to kinetic energy $P^2/2M$.

Fig. 2 (A) Condensate before the application of a Raman pulse. (B) $\Delta m = +1$ transition (19) from a 6 μs pulse with $\delta / 2\pi = 6.4\,\mathrm{MHz}$. This detuning is chosen to be slightly larger than the 6.27 MHz resonance frequency to suppress four-photon coupling to the $m = +1$, $4\hbar k\hat{z}$ state (25). (C) $\Delta m = 0$ transition (26) after a 14 μs Raman pulse with equal laser intensities of $25\,\mathrm{mW/cm^2}$. The relative detuning was $\delta/2\pi = -98\,\mathrm{kHz}$ and the polarizations of both lasers were aligned with $\hat{x}$. The diagrams to the right of (B) and (C) show the polarization of the lasers with respect to the local magnetic field. We verified that no transitions occurred when incorrect polarizations were used. (D) The rotating magnetic field zero (circle of death) results in Majorana transitions of an output-coupled condensate fraction in the m = 0 state. The arrow denotes the physical location of the rotating bias field zero. This is a graphic depiction of Majorana transitions.

Fig. 3 Atoms are coupled to both the $m = 0$ and $m = +1$ magnetic sublevels using a single Raman pulse. (A) Magnetic trap is switched off immediately after the Raman pulse. (B) Magnetic trap is held on for 4 ms after the Raman pulse. (C) Shows the transition used and the laser polarizations.

Fig. 4 In Fig. 4A-C, one, three and six 6 μs Raman pulses were applied to the condensate, respectively. (D) Firing 1 μs Raman pulses at the full repetition rate of ~20 kHz imposed by the frequency of the rotating bias field (140 pulses in 7 ms) produces a quasi-continuous atomic beam.

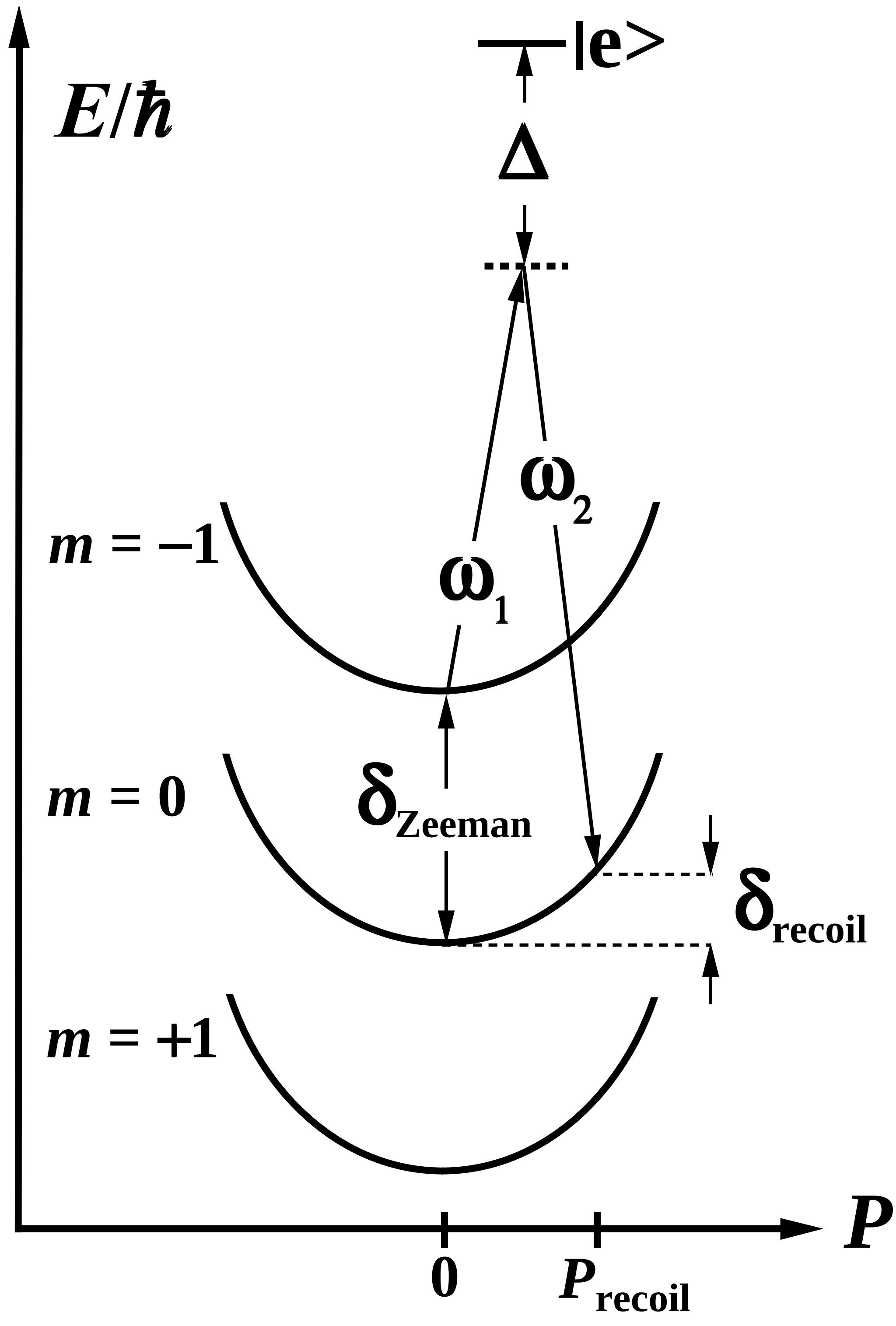

E/ħ
|e>
Δ
ω2
ω1
m = −1
m = 0
m = +1
δZeeman
δrecoil
P
0
Precoil

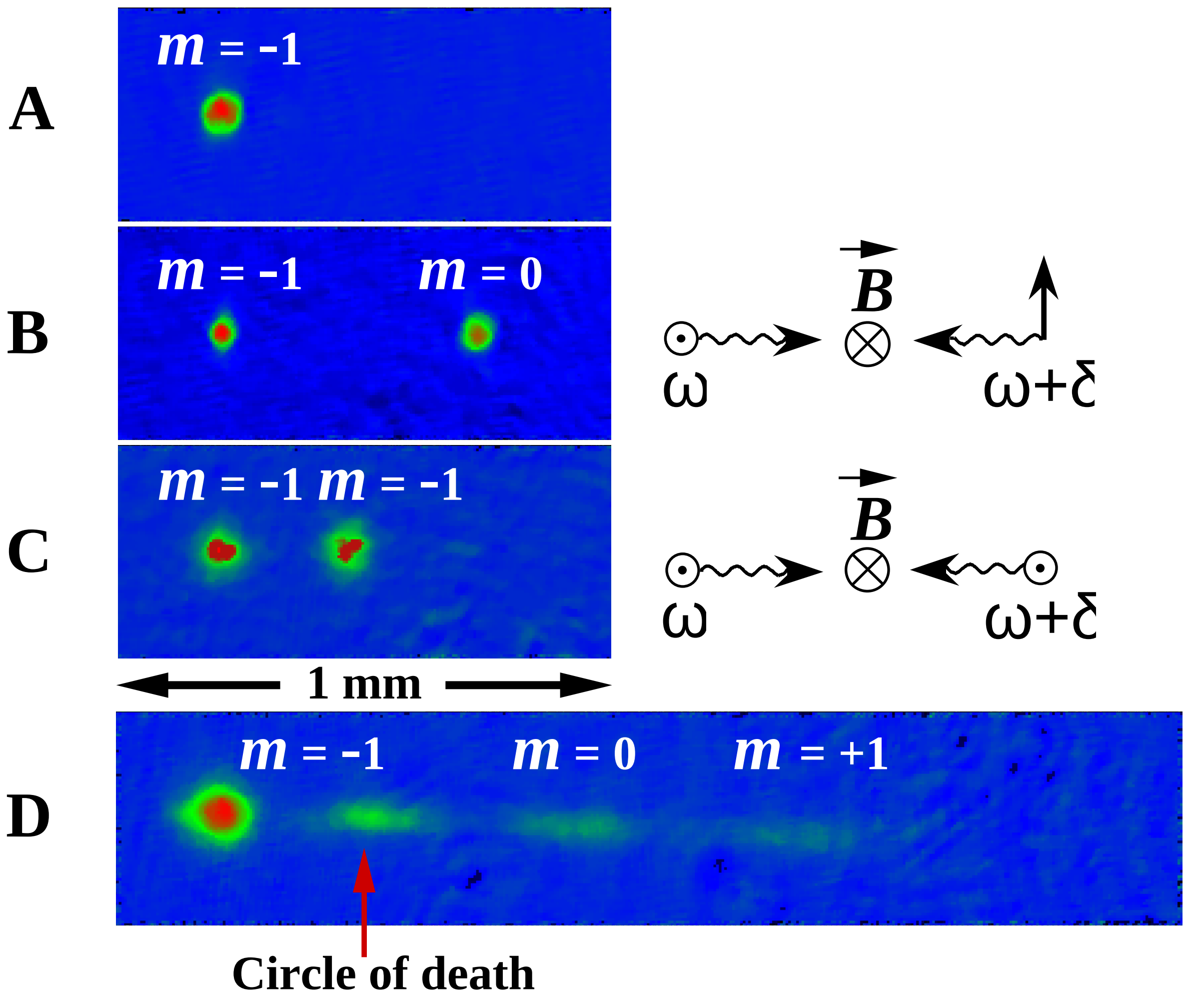
A
m = -1
B
m = -1
m = 0
C
m = -1 m = -1
1 mm
D
m = -1
m = 0
m = +1
Circle of death
B
ω
ω+δ
B
ω
ω+δ

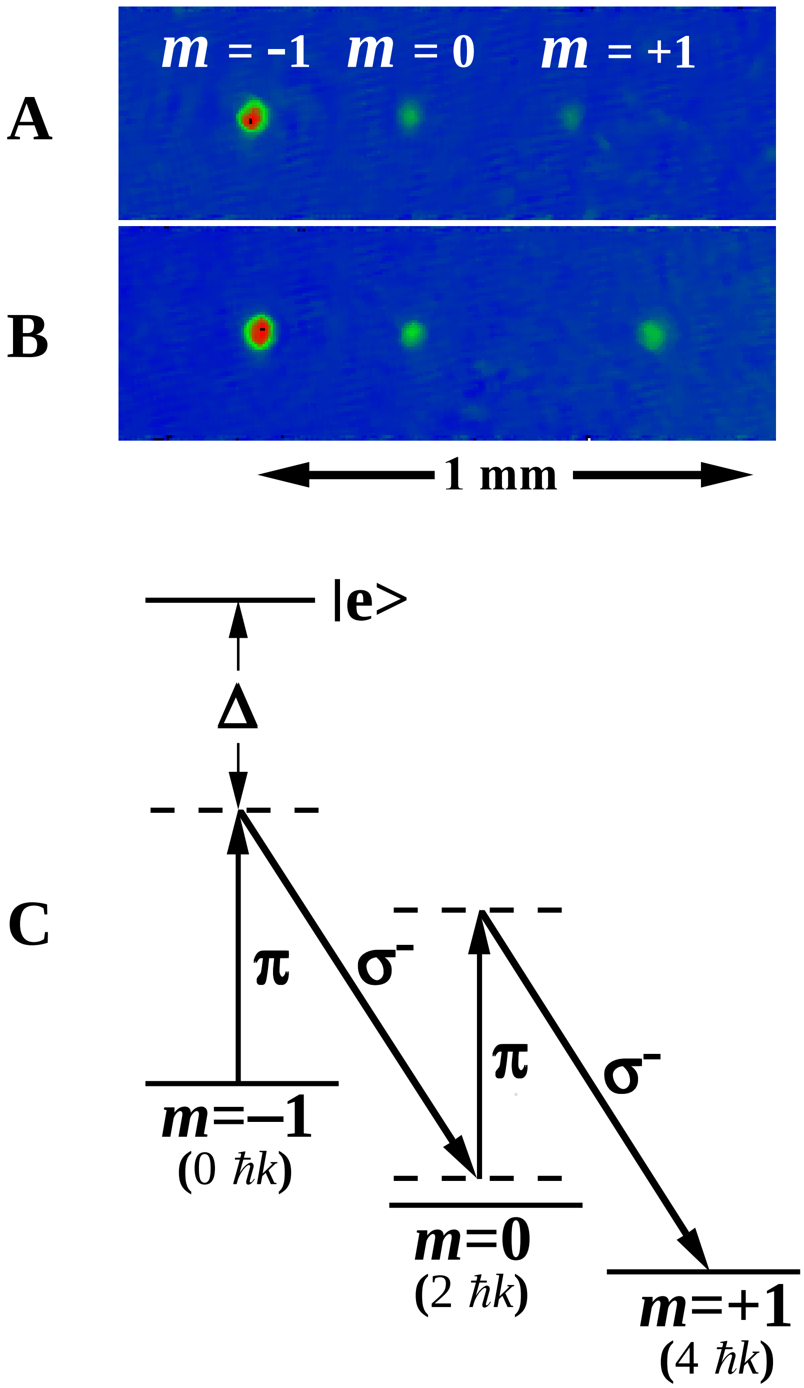

m = -1 m = 0 m = +1
A
B
1 mm
|e>
Δ
C
π
σ-
π
σ-
m=–1
(0 ħk)
m=0
(2 ħk)
m=+1
(4 ħk)

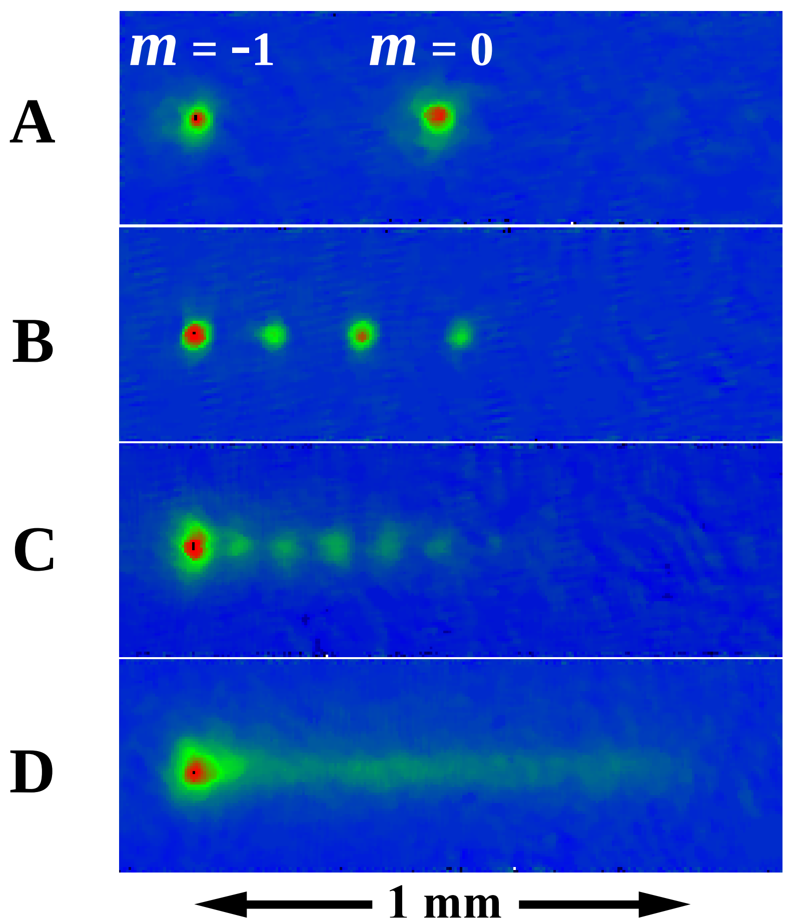

m = -1
m = 0
A
B
C
D
1 mm